

Analysis of a Modified Feedback Control Technique for Suppressing Electrical Alternans in Cardiac Tissue

Srinivasan V. Narayanan¹ and John W. Cain²

¹Dept. of Biomedical Engineering, Virginia Commonwealth University
701 West Grace Street, P.O. Box 843067, Richmond, VA 23284-3067 USA

²Dept. of Mathematics and Center for the Study of Biological Complexity, Virginia Commonwealth University
1001 West Main Street, Richmond, VA 23284-2014 USA

November 27, 2007

ABSTRACT

Alternans is an abnormal cardiac rhythm in which action potential duration alternates from beat-to-beat. In order for an implanted pacemaker to successfully seize control of the heart rhythm, its electrical stimuli have to be carefully timed relative to the firing of the heart's specialized pacemaker cells. In this manuscript, we use mathematical techniques to analyze a novel feedback control algorithm for suppressing alternans. We model the cardiac rhythm and the effect of the controller using a system of two nonlinear difference equations. Our analysis reveals that it is often advantageous *not* to allow the pacemaker to intervene in every beat when attempting to control alternans.

Keywords: Difference equations; Cardiac Arrhythmia; Feedback Control.

1 Introduction

Cardiac arrhythmias kill hundreds of thousands of people in the United States every year. Since the heart's job is to pump oxygenated blood to the body's vital organs, it is not surprising that any rhythm that interferes with pumping performance may be fatal. For example, it is believed that over two-thirds of ventricular fibrillation victims die before even reaching the hospital [32]. Early detection of an arrhythmia can allow time for an implantable pacemaker or defibrillator to intervene, thereby improving the patient's chances of survival.

Mechanical contraction of cardiac muscle occurs in response to electrical signals that propagate through the tissue. To understand the nature of cardiac electrical activity, it is convenient to focus on a single cardiac cell. Positively charged ions such as sodium, potassium, and calcium can pass through channels in the cell membrane. The movement of

ions gives rise to ionic currents through the cell membrane, which in turn cause the transmembrane voltage v to change. In the absence of electrical stimulation, a cell maintains a constant *resting voltage* of about -80 mV by expending energy to pump positively charged ions out of the cell. However, if a sufficiently well-rested cell is stimulated by an electrical current, a sudden and dramatic change in v may result (see Figure 1). Namely, v experiences a rapid rise (upstroke), followed by a prolonged period of elevation (plateau), and finally a recovery phase in which v decreases to the resting voltage while the cell awaits further stimulation. This prolonged elevation of v in response to an electrical stimulus is called an *action potential*. Figure 1 illustrates two consecutive action potentials in a single cardiac cell. For an introduction to mathematical models of the action potential, see [21, 25].

Pacing (repeated stimulation of cardiac tissue) results in a sequence of action potentials. If the interval between consecutive stimuli, or *basic cycle length (BCL)*, is constant, the tissue may exhibit several types of responses:

- *Normal 1:1 response.* Slow pacing (large BCL) generally yields a response in which each action potential is identical (Figure 2a).
- *Alternans.* Faster pacing (smaller BCL) can sometimes cause action potential duration (APD) to alternate in an abnormal long-short pattern (Figure 2b).
- *2:1 response.* After an action potential, a cardiac cell requires a certain amount of recovery time before it can generate another action potential. Very rapid pacing (small BCL) can lead to an abnormal pattern in which the cell “ignores” every other stimulus. We will not consider 2:1 responses in this study.

Alternans is viewed as a precursor to deadly arrhythmias [10, 20, 24, 26, 27, 31], and therefore it is desirable to suppress alternans by using a computerized pacemaker to control the beating of the heart.

One method of controlling alternans is a feedback control technique known as *extended time-delay auto-synchronization (ETDAS)* [28, 29]. Despite the daunting name, ETDAS is based upon a relatively simple idea: by making small adjustments to the timing of the electrical stimuli, the amplitude of APD alternation can be gradually diminished, leading to a normal response in which all APD values are identical (as in Figure 2a). Special cases of ETDAS have been used to control alternans experimentally [7, 8, 16, 17].

It is important to note that an implanted pacemaker (henceforth, the *controller*) must compete with the heart’s native electrical stimuli in order to gain control of the rhythm. In an intact heart, stimuli are usually supplied by a cluster of specialized pacemaker cells known as the *sino-atrial (SA) node*. The SA node sets the BCL, and it is not possible to prolong the interval between stimuli [7, 11]. In other words, the controller is restricted in that it must always preempt the stimuli from the SA node. Mathematically, this imposes a constraint on the ETDAS control algorithm in that lengthening the BCL is not allowed.

In this study, we analyze a modified version of the ETDAS technique in which the controller can be turned off during beats that would require lengthening BCL. Prior studies [7, 12, 15] suggest that the control domain (i.e., the range of system parameters for which the controller successfully suppresses alternans) is actually *larger* if the algorithm is restricted to allow only shortening of the BCL. Through numerical simulations, we find that it is often advantageous if the controller does *not* intervene in every beat. We observe various on/off patterns for the controller—in particular, it is easy to choose ETDAS parameters in such a way that the controller exhibits (i) an on-off pattern in which the controller intervenes in every other beat; (ii) an on-off-off pattern in which the controller intervenes in every third beat; and (iii) a pattern in which the controller intervenes in every beat. Additionally, we expand upon a prior mathematical analysis [2] of ETDAS in that case that the controller is always on.

The remainder of the paper is organized as follows. In Section 2, we provide a background on *restitution*, a feature of cardiac tissue that forms the basis of our model of paced tissue dynamics. Because we use a discrete model of the beating heart, Section 3 includes a brief overview of the analysis of discrete systems. Specifically, we discuss local stability of fixed points of mappings and explain how these mathematical results can be applied in the present context of alternans control. Section 4 introduces the ETDAS technique and provides an algorithm by which this control technique can be used to suppress alternans. We include mathematical analysis of the algorithm, yielding estimates on the ETDAS parameters for which the algorithm succeeds if the controller always remains on. In Section 5, we impose the restriction that the controller is not allowed to lengthen the underlying BCL. Through computer simulations of the model, we determine ranges of the ETDAS parameters for which various on/off controller patterns are observed. Finally, Section 6 includes a brief summary of our findings and a discussion of the limitations of the present study.

2 Background on Cardiac Restitution

We now establish terminology and notation that will be useful in our study of paced cardiac cells. The reader is encouraged to refer to Figure 1 as needed. *Action potential duration (APD)* is defined as the amount of time that v remains elevated above some specified threshold voltage v_{thr} during an action potential. The *diastolic interval (DI)* is the amount of recovery time during which $v < v_{\text{thr}}$ between consecutive action potentials. When mathematical notation is required, we will use the symbols in Table 1 (see also Figure 1). Observe that $B_n = A_n + D_n$ represents the amount of time between the n th and $(n + 1)$ th stimuli. In situations when the pacing interval B_n is constant, we will write $B_n = B$ and refer to this interval as the *basic cycle length (BCL)*.

Generally, the longer the DI, the longer the APD that follows; i.e., more rest yields longer action potentials. This important feature of cardiac cells, known as APD *restitution*, can be

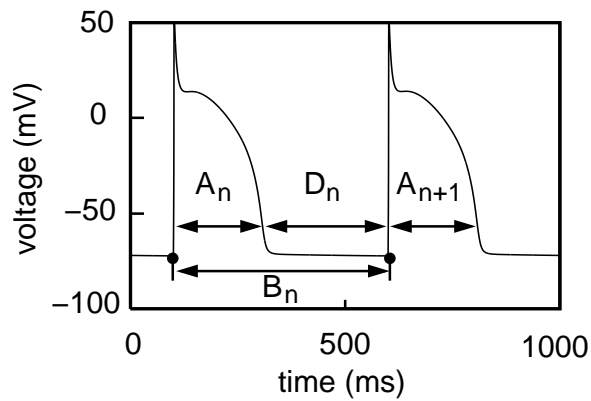


Figure 1: Action potentials generated by numerical simulation of a cardiac membrane model [22]. Stimuli are indicated by bold dots. The notation is explained in Section 2.

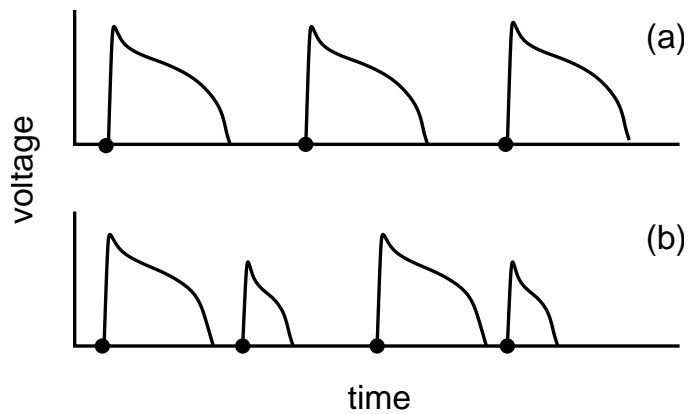


Figure 2: (a) A normal rhythm in which action potential duration is the same in each beat. (b) Alternans. Stimuli are indicated by bold dots.

Symbol	Meaning
A_n	duration of action potential following n th stimulus
D_n	diastolic interval between n th and $(n + 1)$ th action potentials
B_n	interval between n th and $(n + 1)$ th stimuli

Table 1: Notation relating to paced cardiac cells.

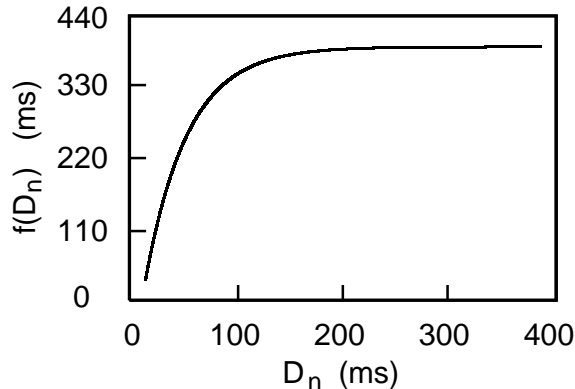


Figure 3: Restitution curve given by Equation (2).

modeled mathematically via the following relationship [23]:

$$A_{n+1} = f(D_n). \quad (1)$$

The function f is known as the *restitution function*, and its graph is called the *restitution curve*. In the remainder of this paper, when simulations are required we will use the restitution function

$$f(D_n) = 392 - 525e^{-D_n/40}, \quad (2)$$

the graph of which appears in Figure 3. This restitution function was used to fit experimentally obtained bullfrog restitution data [17]. For more information on the importance of APD restitution, see for example [1, 3, 5].

3 Mappings, Fixed Points, Stability and Bifurcations

We now provide a brief overview of discrete dynamical systems such as (1). For additional details, see Chapter 10 of Strogatz [30]. In what follows, we will assume that f is a smooth (i.e., repeatedly differentiable) function.

Definition 3.1. Suppose $f : \mathbb{R} \mapsto \mathbb{R}$. A relationship of the form

$$x_{n+1} = f(x_n) \tag{3}$$

is called a *one-dimensional mapping*, or simply a *map*.

Definition 3.2. A *fixed point* of the map (3) is any number x^* such that $x^* = f(x^*)$. We say that a fixed point x^* is *isolated* if there exists $\delta > 0$ such that x^* is the only fixed point in the open interval $(x^* - \delta, x^* + \delta)$.

A fixed point of a map is analogous to an equilibrium of an ordinary differential equation and, like equilibria, fixed points can be either attractors or repellers. If we start from an initial point x_0 that is “close” to a fixed point x^* , it is natural to ask whether the subsequent iterates of (3) converge to x^* or are repelled by x^* . The following Lemma, the proof of which appears in Strogatz ([30], page 349–350), provides a stability criterion for fixed points of one-dimensional mappings:

Lemma 3.3. (Stability Criterion) *A fixed point x^* of the mapping (3) is a local attractor if $|f'(x^*)| < 1$ and a repeller if $|f'(x^*)| > 1$. If $|f'(x^*)| = 1$, this stability test is inconclusive.*

For example, note that the mapping $x_{n+1} = x_n^2$ has two fixed points: $x^* = 0$ and $x^* = 1$. In this case, $f(x) = x^2$ and therefore $f'(x) = 2x$. Since $|f'(0)| = 0 < 1$, we conclude that 0 is an attractor and, since $|f'(1)| = 2 > 1$, we conclude that 1 is a repeller. We remark that the stability criterion given by this Lemma is *local*. Indeed, iterates of this mapping are only attracted to 0 if the initial condition satisfies $x_0 \in (-1, 1)$.

One-dimensional mappings of the form $x_{n+1} = f(x_n; \mu)$ where μ is a parameter may exhibit a wide range of dynamical behavior. For example, let μ be a parameter between 0 and 4 and consider the *discrete logistic mapping*

$$x_{n+1} = f(x_n) = \mu x_n(1 - x_n). \tag{4}$$

The reader will verify that this mapping has two fixed points: $x^* = 0$ and $x^* = 1 - \mu^{-1}$. The former is an attractor if $0 < \mu < 1$ and a repeller otherwise. The latter is an attractor if $1 < \mu < 3$ and a repeller otherwise. Since both fixed points are unstable for $\mu > 3$, one may ask what would happen if the mapping (4) is iterated for such values of μ . For $3 < \mu < 1 + \sqrt{6}$, one may show [30] that the mapping (4) has a stable 2-cycle. Indeed, if $x_0 \in [0, 1] \setminus \{0, 1 - \mu^{-1}\}$, the iterates of (4) converge to a pattern of alternation between two values. For $1 + \sqrt{6} < \mu < 3.544\dots$, the mapping has a stable 4-cycle. We say that *period-doubling bifurcations* occur at $\mu = 3$ and $\mu = 1 + \sqrt{6}$. As explained in Strogatz [30], this period-doubling cascade continues until $\mu = 1 + \sqrt{8}$, at which point chaos ensues.

3.1 Application to Paced Cardiac Cells

As pacing becomes more rapid, alternans is sometimes initiated via a period-doubling bifurcation [13]. To see how, suppose that we pace with a constant period $B_n = B$. Since

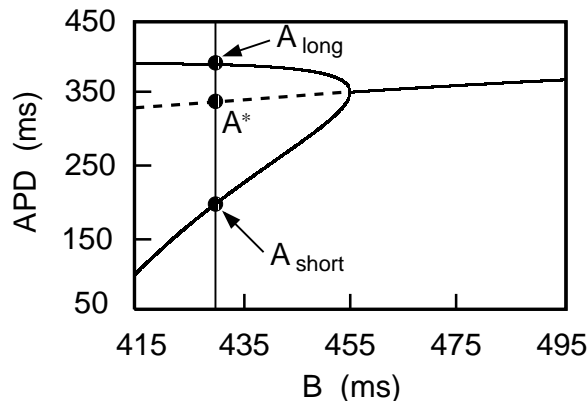


Figure 4: Bifurcation to alternans. For each fixed $B < 455$ ms, the iterates of the mapping (5) alternate between long and short values, as illustrated for $B = 430$ ms.

$A_n + D_n = B$ for all n , Equation (1) can be rewritten as

$$A_{n+1} = f(B - A_n). \quad (5)$$

Assuming that f is qualitatively similar to the function shown in Figure 3, it is easy to argue that the mapping (5) has a unique fixed point A^* satisfying $A^* = f(B - A^*)$. By Lemma 3.3, the fixed point is an attractor if $|f'(B - A^*)| < 1$. Inspecting Figure 3, one expects that this criterion is satisfied if B is large, and this is indeed the case. However, as B is decreased, we reach a point at which the slope of the restitution curve exceeds 1 at $(B - A^*)$. The mapping (5) experiences a period-doubling bifurcation, resulting in alternans. Figure 4 shows a bifurcation diagram for the mapping (5), using the restitution function given by Equation (2). For $B > 455$ ms, the fixed point of (5) is an attractor. A period-doubling bifurcation occurs at $B = 455$ ms, leading to alternans at shorter values of B . Observe that the amplitude of alternans is small near the bifurcation point but becomes much larger as B decreases.

3.2 Systems of Mappings

More generally, consider a *system* of two mappings of the form

$$\begin{aligned} x_{n+1} &= \Phi_1(x_n, y_n) \\ y_{n+1} &= \Phi_2(x_n, y_n), \end{aligned} \quad (6)$$

where x_n and y_n are real numbers. Note that this system maps the *vector* (x_n, y_n) to the *vector* (x_{n+1}, y_{n+1}) .

Definition 3.4. A *fixed point* of the system (6) is a vector (x^*, y^*) such that $x^* = \Phi_1(x^*, y^*)$ and $y^* = \Phi_2(x^*, y^*)$. The fixed point is *isolated* if there exists $\delta > 0$ such that the open disc of radius δ centered at (x^*, y^*) contains no other fixed points.

We now wish to develop a stability criterion analogous to Lemma 3.3 for a fixed point (x^*, y^*) of the system (6). To do so, we replace Φ_1 and Φ_2 by their tangent plane approximations in the vicinity of the fixed point. That is,

$$\Phi_1(x, y) \approx \Phi_1(x^*, y^*) + \frac{\partial \Phi_1}{\partial x}(x^*, y^*) \cdot (x - x^*) + \frac{\partial \Phi_1}{\partial y}(x^*, y^*) \cdot (y - y^*) \quad (7)$$

$$\Phi_2(x, y) \approx \Phi_2(x^*, y^*) + \frac{\partial \Phi_2}{\partial x}(x^*, y^*) \cdot (x - x^*) + \frac{\partial \Phi_2}{\partial y}(x^*, y^*) \cdot (y - y^*). \quad (8)$$

Now since (x^*, y^*) is a fixed point, we may replace $\Phi_1(x^*, y^*) = x^*$ and $\Phi_2(x^*, y^*) = y^*$ in Equations (7)–(8). Inserting (7)–(8) into Equation (6) and introducing matrix notation, we obtain the following linear approximation of our original system:

$$\begin{bmatrix} x_{n+1} - x^* \\ y_{n+1} - y^* \end{bmatrix} \approx \begin{bmatrix} \frac{\partial \Phi_1}{\partial x}(x^*, y^*) & \frac{\partial \Phi_1}{\partial y}(x^*, y^*) \\ \frac{\partial \Phi_2}{\partial x}(x^*, y^*) & \frac{\partial \Phi_2}{\partial y}(x^*, y^*) \end{bmatrix} \begin{bmatrix} x_n - x^* \\ y_n - y^* \end{bmatrix}. \quad (9)$$

Observe that Equation (9) expresses how “close” we are to the fixed point (x^*, y^*) at the $(n + 1)$ st time step in terms of how “close” we are to the fixed point at the n th time step.

Definition 3.5. Define the function $\Phi : \mathbb{R}^2 \mapsto \mathbb{R}^2$ by

$$\Phi(x, y) = \begin{bmatrix} \Phi_1(x, y) \\ \Phi_2(x, y) \end{bmatrix}.$$

The 2×2 matrix appearing in Equation (9) is called the *Jacobian matrix* of Φ evaluated at (x^*, y^*) . We will denote this matrix by $\mathbf{J}\Phi(x^*, y^*)$.

The Jacobian matrix is a higher-dimensional analogue of the derivative of a function $f : \mathbb{R} \mapsto \mathbb{R}$. Consequently, it is not surprising that the stability criterion for fixed points of systems of mappings involves $\mathbf{J}\Phi(x^*, y^*)$, much as the stability criterion for the mapping (3) involved a derivative $f'(x^*)$ (see Lemma 3.3).

Lemma 3.6. (Stability Criterion for Systems). *Suppose (x^*, y^*) is an isolated fixed point of the system (6), and let λ_1 and λ_2 denote the eigenvalues of the Jacobian matrix $\mathbf{J}\Phi(x^*, y^*)$. Then the fixed point is a local attractor if both $|\lambda_1| < 1$ and $|\lambda_2| < 1$. The fixed point is a repeller if either $|\lambda_1| > 1$ or $|\lambda_2| > 1$. Here, $|\cdot|$ denotes modulus.*

Ultimately, we wish to apply Lemma 3.6 to a particular system of mappings that model control of the cardiac rhythm with an implanted pacemaker (see Section 4.2). In doing so, we wish to determine how the choice of parameters affects the stability of the targeted (i.e., normal) rhythm. Fortunately, there is a simple test [19] for whether all eigenvalues of a matrix have modulus less than one. We state this result for the special case of 2×2 matrices.

Lemma 3.7. (Jury Stability Test). *Suppose J is any 2×2 matrix, and let T and Δ denote the trace and determinant of J , respectively. Then both eigenvalues of J have modulus less than 1 if and only if (i) $T - \Delta < 1$, (ii) $T + \Delta > -1$, and (iii) $\Delta < 1$.*

In the next section, we describe the ETDAS method of feedback control and apply Lemmas 3.6–3.7 to predict ranges of parameter values for which control is likely to suppress alternans.

4 Controlling Alternans with ETDAS

Suppose a cell is paced with period B , resulting in alternans. To suppress alternans, we will adjust B during each beat, choosing the “adjustments” in such a way that the sequence $\{A_n\}$ converges to the fixed point A^* as $n \rightarrow \infty$. If we let ϵ_n denote the adjustment to the n th inter-stimulus interval, then we may write $B_n = B + \epsilon_n$. The mapping (5) is modified to read

$$A_{n+1} = f(B + \epsilon_n - A_n). \quad (10)$$

There are many possible ways to choose ϵ_n —we will use a method known as *extended time-delay auto-synchronization (ETDAS)* [2, 28, 29]:

$$\epsilon_{n+1} = \gamma (A_{n+1} - A_n) + R\epsilon_n. \quad (11)$$

Here, the non-negative parameter γ is called the *feedback gain*, and provides a measure of the “strength” of the control. We refer to the non-negative parameter R as the *history parameter* because it measures how much weight or influence past APD values have on the controller. In the following subsection, we use Equations (10)–(11) to present an algorithm for controlling alternans.

4.1 Computer Simulations with ETDAS

Figure 5 shows the results of computer “experiments” in which the ETDAS algorithm is used to control alternans as follows. First, we induce alternans by iterating the mapping (5) with $B = 430$, using the restitution function (3). Choosing the initial value $A_0 = 200$, the iterates rapidly settle into an alternating pattern between two values, A_{short} and A_{long} . After

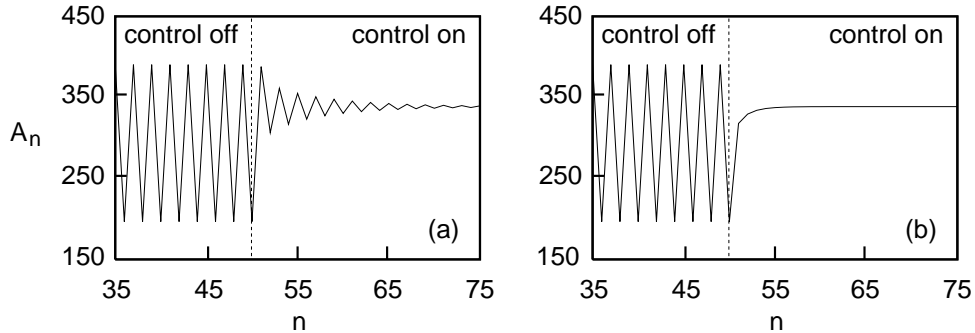


Figure 5: Initiation of ETDAS control after 50 beats of alternans (see text for details). (a) $R = \gamma = 0.2$. Note that the sequence A_n alternates about A^* as the convergence takes place. (b) $R = \gamma = 0.8$. After control is initiated, A_n increases monotonically to A^* .

iterating Equation (5) for 50 beats (regions labeled “control off” in Figure 5), we find that $A_{50} = A_{\text{short}} = 196.473$. After the 50th beat, we suddenly initiate control by switching from Equation (5) to Equations (10) and (11), using particular choices of the parameters R and γ . (Note: In order to start the algorithm, we use $\epsilon_{49} = 0$). Figure 5a illustrates the sequence of APD values if $R = \gamma = 0.2$. In this case, ETDAS succeeds in stopping alternans and the iterates exhibit damped oscillation as they converge to $A^* = 338.587$. Figure 5b shows the sequence of APD values if $R = \gamma = 0.8$. Again, ETDAS stops alternans, but this time the iterates increase monotonically to A^* after control is turned on. The reason for distinguishing between the two types of convergence shown in Figure 5 will be explained in the next section.

4.2 Mathematical Analysis of ETDAS

Using Lemmas 3.6–3.7, we can determine ranges of the parameters γ and R for which the ETDAS algorithm successfully suppresses alternans. As usual, we let B denote the underlying BCL and assume that A^* is the corresponding fixed point of (5). We rewrite Equations (10)–(11) in the form of the systems discussed in Section 3.2 above:

$$\begin{aligned}
 A_{n+1} &= f(B + \epsilon_n - A_n) \\
 \epsilon_{n+1} &= \gamma [f(B + \epsilon_n - A_n) - A_n] + R\epsilon_n.
 \end{aligned}
 \tag{12}$$

Observe that the vector $(A^*, 0)$ is a fixed point of this system. If $\gamma = R = 0$ (i.e., if the controller is off), we would expect this fixed point to be unstable for values of B that promote alternans. More generally, we may characterize the values of γ and R for which the fixed point is stable:

Theorem 4.1. *Let $s = f'(B - A^*)$. Then the fixed point $(A^*, 0)$ of the system (12) is a (local) attractor if both $0 \leq R < 1$ and*

$$\left(\frac{R+1}{2}\right) \left(1 - \frac{1}{s}\right) < \gamma < R + \frac{1}{s}. \quad (13)$$

Note that s represents a slope of the restitution curve.

Proof. According to Lemma 3.6, we must compute the Jacobian matrix \mathbf{J} associated with the system (12), and evaluate it at the fixed point $(A^*, 0)$. Computing all the necessary partial derivatives, we find that

$$\mathbf{J} = \begin{bmatrix} -f'(B - A^*) & f'(B - A^*) \\ -\gamma[f'(B - A^*) + 1] & \gamma f'(B - A^*) + R \end{bmatrix} = \begin{bmatrix} -s & s \\ -\gamma(s + 1) & \gamma s + R \end{bmatrix}. \quad (14)$$

The trace T and determinant Δ of \mathbf{J} are given by

$$T = s(\gamma - 1) + R \quad \text{and} \quad \Delta = (\gamma - R)s. \quad (15)$$

Invoking Lemma 3.7 with T and Δ from (15), we see that requiring $T - \Delta < 1$ yields the restriction $R < 1$. Similarly, straightforward algebra reveals that the lower inequality in (13) follows from requiring $T + \Delta > -1$, and the upper inequality in (13) follows from requiring $\Delta < 1$. Finally, the restriction $R \geq 0$ is a consequence of our earlier assumption that R is a non-negative parameter. \square

Although Theorem 4.1 provides some insight as to what parameters we should use when implementing the ETDAS algorithm experimentally, in the next section we shall see that inequality (13) alone is not sufficient to guarantee that ETDAS successfully controls alternans in a patient's heart.

5 Restricting the Controller

The implanted controller must compete with the heart's specialized pacemaker cells for control of the rhythm. Assuming that the tissue is sufficiently well-rested, the first stimulus that arrives at a given cell is the one that will initiate the action potential. Therefore, in order for the controller to take over the rhythm, it must preempt the heart's native electrical stimuli [2, 7, 8]. Mathematically, this means that we should require $\epsilon_n \leq 0$ for all n .

Unfortunately, unless both R and γ are chosen large (i.e., close to 1), the ETDAS method often generates positive values for ϵ_n . For example, suppose we iterate Equations (10)–(11) using $B = 430$ and $R = \gamma = 0.2$. Recall from Figure 5a that the sequence $\{A_n - A^*\}$

alternates as it converges to zero. The corresponding values of ϵ_n after initiation of control are as follows:

$$31.9518, -9.69696, 8.47417, -6.78803, 5.95701, -4.93954, 4.33664, -3.658\dots$$

Observe that every other number in this sequence is positive.

One way to avoid the issue of positive ϵ_n values is to simply turn the controller off during beats that would require $\epsilon_n > 0$. Several prior studies [7, 12, 15] suggest that doing so is advantageous because it enlarges the range of parameter values for which feedback control succeeds. Equation (11) is easily modified to yield the *restricted ETDAS* equation:

$$\epsilon_{n+1} = \min \{0, \gamma (A_{n+1} - A_n) + R\epsilon_n\}. \quad (16)$$

The only difference between Equations (11) and (16) is that by taking the minimum in (16), we do not allow for positive values of ϵ_n . In the following subsection, we show results of numerical simulations of Equations (10), (16).

5.1 Computer Simulations

We performed numerical simulations of the restricted ETDAS algorithm to determine how R and γ affect the on/off pattern of the controller. The details of the simulations are as follows: First, alternans was initiated by iterating Equation (5) with $BCL = 430$ for 100 beats, using the restitution function in Equation (2). The resulting sequence of APD values alternated between 196.473 and 390.469. After the 100th beat (a short action potential), we suddenly turned on restricted ETDAS control—that is, we switched from Equation (5) to Equation (10), with ϵ_n given by (16) for particular choices of R and γ . To help determine the on/off pattern of the controller, we iterated Equations (10), (16) for many beats and computed the percentage of beats in which the controller was turned on (i.e., the percentage of beats in which Equation (16) returns a strictly negative number). This entire process was repeated for various choices of R and γ —specifically, both parameters ranged from 0 to 1 in steps of 0.01, yielding a total of 10000 data points.

The results of the simulations are displayed in Figure 6, which shows a color-coded plot of the percentage of beats in which the restricted ETDAS algorithm (16) determined that the controller should be on. Notably, the figure can be divided (roughly) into three large zones, each with a corresponding on/off pattern for the controller. For small R and large γ (upper left corner, dark blue), the controller should be turned on in every third beat, resulting in an on-off-off pattern. Much of the light blue region corresponds to an on-off pattern in which the controller should be turned on in every other beat. For large R and γ (upper right corner, dark red), the controller should be turned on in every beat (i.e., $\epsilon_n < 0$ for all n). Other patterns may be possible, as indicated by other colors in the plot. Table 2 summarizes the three most common patterns exhibited by the controller, and lists sample parameter values that can be used to generate those patterns.

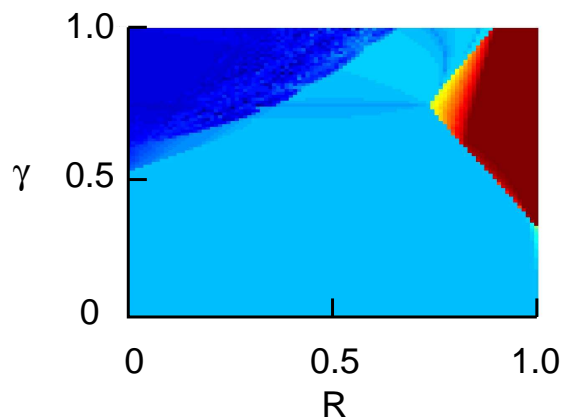


Figure 6: Color-coded plot of percentage of beats in which the controller is on. The dark blue region in the upper-left corner corresponds to the on-off-off pattern (i.e., controller on $33\frac{1}{3}$ % of the time). Much of the light blue region corresponds to an on-off pattern, and the dark red region corresponds to a pattern in which the controller is always on.

R	γ	controller pattern
0.2	0.2	101010101010
0.1	0.9	100100100100
0.85	0.85	111111111111

Table 2: On/off patterns for the controller for various choices of the ETDAS parameters. From top to bottom: (i) Controller active in every other beat; (ii) Controller active in every third beat; (iii) Controller active in every beat.

6 Discussion and Conclusions

When a cardiac cell experiences alternans, it is possible to apply carefully timed electrical stimuli in such a way that the cell resumes a normal rhythm. We have analyzed a particular algorithm, known as ETDAS, for determining when an implanted pacemaker should intervene by applying stimuli. By exploiting the feature of cardiac tissue known as APD restitution, we derived conditions (Theorem 4.1) that ETDAS parameters must satisfy in order for the algorithm to succeed. However, since the stimuli applied by the controller must preempt the heart’s native electrical stimuli, our algorithm must be constrained to obey $\epsilon_n \leq 0$ for all n (see Section 5). Hence, Theorem 4.1 alone is not enough to characterize the set of ETDAS parameters for which the algorithm would successfully stop alternans experimentally. We address this problem by introducing the *restricted ETDAS algorithm* (Equation (16)), which allows the controller to be turned off during beats that would require $\epsilon_n > 0$. We find that the restricted ETDAS algorithm produces several distinct on/off patterns as illustrated in Figure 6 and Table 2. Notably, for most choices of parameters, it is to our advantage *not* to let the controller intervene during every beat.

Limitations: One limitation of the present study concerns our assumption that APD restitution can be modeled by a simple mapping of the form (5). In some circumstances, such a mapping provides a reasonably accurate description of a paced cell. However, cardiac cells exhibit *memory* in the sense that A_{n+1} depends upon the recent pacing history of the cell, not just the preceding DI. In other words, it may be more realistic to model restitution with a mapping of the form

$$A_{n+1} = f(D_n, A_n, D_{n-1}, A_{n-1}, \dots, D_{n-k}, A_{n-k}), \quad (17)$$

where k provides a measure of how much “memory” the cell has. We remark that the ETDAS control algorithm can still be used even if a memory model such as (17) is used. However, extending the analysis of Section 4.2 is not as straightforward. For more information on short-term memory of cardiac cells and its implications, see [4, 6, 14].

Another limitation of the present study is that we consider only *local* control—that is, we seek to control alternans in a single cell (or small patch of cells). However, each cardiac cell is (electrically) coupled to its neighboring cells, and thus it is not clear that controlling alternans locally is sufficient to prevent alternans from occurring elsewhere in the heart. Several studies [9, 18] suggest that feedback control algorithms such as ETDAS can only terminate alternans in the immediate vicinity of the implanted pacemaker electrode. Fortunately, the restricted ETDAS algorithm discussed here is quite robust relative to other feedback control algorithms [2], and this may help reduce the number of local controllers needed to terminate alternans in the whole heart.

Finally, concerning Figure 6, we should point out that the percentage of beats in which the controller is on provides only a rough measure of the underlying on/off pattern for the

controller. To truly identify the controller’s on/off pattern, one must carefully inspect the values of ϵ_n that are generated by the restricted ETDAS algorithm. For example, certain parts of the orange region in Figure 6 correspond to a sustained on-on-off pattern, while other parts of the orange region correspond to situations in which the controller is initially always on, but eventually settles into an on-off pattern. Another complication arises from the computer’s limited precision—namely, for certain choices of R and γ , the convergence from alternans to a normal rhythm is so rapid that $|\epsilon_n| < 10^{-14}$ within a few dozen beats. However, since double precision arithmetic on most desktop computers is accurate only to about 10^{-14} , it is likely that some of the patterns encoded in Figure 6 are merely consequences of the computer’s limited accuracy. A more thorough study of the possible on/off patterns would likely require (i) using higher precision arithmetic and (ii) automating the computer to identify the long-term on/off pattern of the controller.

Acknowledgments

We gratefully acknowledge the financial support of the Honors Summer Undergraduate Research Program at Virginia Commonwealth University.

References

- [1] I. BANVILLE AND R. A. GRAY, *Effect of action potential duration and conduction velocity restitution and their spatial dispersion on alternans and the stability of arrhythmias*, J. Cardiovasc. Electrophysiol., 13 (2002), pp. 1141–1149.
- [2] C. M. BERGER, J. W. CAIN, J. E. S. SOCOLAR AND D. J. GAUTHIER, *Control of electrical alternans in simulations of paced myocardium using extended time-delay autosynchronization*, Phys. Rev. E, 76 (2007), pp. 041917.
- [3] M. R. BOYETT AND B. R. JEWELL, *A study of the factors responsible for rate-dependent shortening of the action potential in mammalian ventricular muscle*, J. Physiol., 285 (1978), pp. 359–380.
- [4] J. W. CAIN, E. G. TOLKACHEVA, D. G. SCHAEFFER AND D. J. GAUTHIER, *Rate-dependent propagation of cardiac action potentials in a one-dimensional fiber*, Phys. Rev. E, 70 (2004), pp. 061906.
- [5] J. CAO, Z. QU, Y. KIM, T. WU, A. GARFINKEL, J. N. WEISS, H. S. KARAGUEUZIAN AND P. CHEN, *Spatiotemporal heterogeneity in the induction of ventricular fibrillation by rapid pacing: importance of cardiac restitution properties*, Circ. Res., 84 (1999), pp. 1318–1331.

- [6] E. M. CHERRY AND F. H. FENTON, *Suppression of alternans and conduction blocks despite steep APD restitution: electrotonic, memory, and conduction velocity restitution effects*, Am. J. Physiol., 286 (2004), pp. H2332–H2341.
- [7] D. J. CHRISTINI, M. L. RICCIO, C. A. CULIANU, J. J. FOX, A. KARMA, AND R. F. GILMOUR, JR., *Control of electrical alternans in canine Purkinje fibers*, Phys. Rev. Lett., 96 (2006), pp. 104101.
- [8] D. J. CHRISTINI, K. M. STEIN, S. M. MARKOWITZ, S. MITTAL, D. J. SLOTWINER, M. A. SCHEINER, S. IWAI, AND B. B. LERMAN, *Nonlinear-dynamical arrhythmia control in humans*, Proc. Natl. Acad. Sci., 98 (2001), pp. 5827–5832.
- [9] B. ECHEBARRIA AND A. KARMA, *Instability and spatiotemporal dynamics of alternans in paced cardiac tissue*, Phys. Rev. Lett., 88 (2002), pp. 208101.
- [10] F. H. FENTON, E. M. CHERRY, H. M. HASTINGS AND S. J. EVANS, *Multiple mechanisms of spiral wave breakup in a model of cardiac electrical activity*, Chaos, 12 (2002), pp. 852–892.
- [11] A. GARFINKEL, M. L. SPANO, W. L. DITTO AND J. N. WEISS, *Controlling cardiac chaos*, Science, 257 (1992), pp. 1230–1235.
- [12] D. J. GAUTHIER AND J. E. S. SOCOLAR, *Comment on, “Dynamic Control of Cardiac Alternans”*, Phys. Rev. Lett., 79 (1997), pp. 4938.
- [13] M. R. GUEVARA, G. WARD, A. SHRIER AND L. GLASS, in *Proceedings of the 11th Computers in Cardiology Conference*, IEEE Computer Society, Los Angeles, 1984, pp. 167.
- [14] G. M. HALL, S. BAHAR AND D. J. GAUTHIER, *Prevalence of rate-dependent behaviors in cardiac muscle*, Phys. Rev. Lett., 82 (1999), pp. 2995–2998.
- [15] K. HALL AND D. J. CHRISTINI, *Restricted feedback control of one-dimensional maps*, Phys. Rev. E, 63 (2001), pp. 046204.
- [16] K. HALL, D. J. CHRISTINI, M. TREMBLAY, J. J. COLLINS, L. GLASS, AND J. BILLETTE, *Dynamic control of cardiac alternans*, Phys. Rev. Lett., 78 (1997), pp. 4518–4521.
- [17] G. M. HALL AND D. J. GAUTHIER, *Experimental control of cardiac muscle alternans*, Phys. Rev. Lett., 88 (2002), pp. 198102.
- [18] P. N. JORDAN AND D. J. CHRISTINI, *Adaptive diastolic interval control of cardiac action potential duration alternans*, J. Cardiovasc. Electrophysiol., 15 (2004), pp. 1177–1185.

- [19] E. I. JURY AND J. BLANCHARD, In: *Proceedings of the IRE*, 49 (1961), pp. 1947–1948.
- [20] A. KARMA, *Spiral breakup in model equations of action potential propagation in cardiac tissue*, *Phys. Rev. Lett.*, 71 (1993), pp. 1103–1107.
- [21] J. P. KEENER AND J. SNEYD, *Mathematical Physiology*, Springer-Verlag, New York, 1998.
- [22] C. H. LUO AND Y. RUDY, *A model of the ventricular cardiac action potential: Depolarization, repolarization, and their interaction*, *Circ. Res.*, 68 (1991), pp. 1501–1526.
- [23] J. B. NOLASCO AND R. W. DAHLEN, *A graphic method for the study of alternation in cardiac action potentials*, *J. Appl. Physiol.*, 25 (1968), pp. 191–196.
- [24] J. M. PASTORE, S. D. GIROUARD, K. R. LAURITA, F. G. AKAR AND D. S. ROSENBAUM *Mechanism linking T-wave alternans to the genesis of cardiac fibrillation*, *Circulation*, 99 (1999), pp. 1499–1507.
- [25] R. PLONSEY AND R. C. BARR, *Bioelectricity: A Quantitative Approach*, Plenum Press, New York, 1988.
- [26] D. S. ROSENBAUM, P. ALBRECHT AND R. J. COHEN, *Predicting sudden cardiac death from T wave alternans of the surface electrocardiogram: promise and pitfalls*, *J. Cardiovasc. Electrophysiol.*, 7 (1996), pp. 1095–1111.
- [27] D. S. ROSENBAUM, L. E. JACKSON, J. M. SMITH, H. GARAN, J. N. RUSKIN AND R. J. COHEN, *Electrical alternans and vulnerability to ventricular arrhythmias*, *New Engl. J. Medicine*, 330 (1994), pp. 235–241.
- [28] J. E. S. SOCOLAR AND D. J. GAUTHIER, *Analysis and comparison of multiple-delay schemes for controlling unstable fixed points of discrete maps*, *Phys. Rev. E*, 57 (1998), pp. 6589–6595.
- [29] J. E. S. SOCOLAR, D. W. SUKOW AND D. J. GAUTHIER, *Stabilizing unstable periodic orbits in fast dynamical systems*, *Phys. Rev. E*, 50 (1994), pp. 3245–3248.
- [30] S. STROGATZ, *Nonlinear Dynamics and Chaos*, Perseus, Cambridge, 1994.
- [31] M. A. WATANABE, F. H. FENTON, S. J. EVANS, H. M. HASTINGS AND A. KARMA, *Mechanisms for discordant alternans*, *J. Cardiovasc. Electrophys.*, 12 (2001), pp. 196–206.
- [32] http://www.hrspatients.org/patients/heart_disorders/cardiac_arrest/
(Information accessed in August 2007.)